Chemico-Biological Interactions 181 (2009) 359–365

Contents lists available at ScienceDirect

Chemico-Biological Interactions

journal homepage: www.elsevier.com/locate/chembioint

Generation of oxidant response to copper and iron nanoparticles and salts: Stimulation by ascorbate

Robert H. Rice[a,*], Edgar A. Vidrio[b], Benjamin M. Kumfer[c], Qin Qin[a], Neil H. Willits[d], Ian M. Kennedy[c], Cort Anastasio[b]

[a] Department of Environmental Toxicology, University of California, Davis, CA 95616, United States
[b] Department of Air Land and Water Resources, University of California, Davis, CA 95616, United States
[c] Department of Mechanical and Aeronautical Engineering, University of California, Davis, CA 95616, United States
[d] Department of Statistics, University of California, Davis, CA 95616, United States

ARTICLE INFO

Article history:
Received 19 November 2008
Received in revised form 26 July 2009
Accepted 6 August 2009
Available online 14 August 2009

Keywords:
Heme oxygenase-1
Hydroxyl radical
Human keratinocytes
Nrf2 transcription factor

ABSTRACT

The present work describes a two-stage approach to analyzing combustion-generated samples for their potential to produce oxidant stress. This approach is illustrated with the two commonly encountered transition metals, copper and iron. First, their abilities to generate hydroxyl radical were measured in a cell-free, phosphate-buffered saline solution containing ascorbate and/or citrate. Second, their abilities to induce heme oxygenase-1 in cultured human epidermal keratinocytes were assessed in cell culture. Combustion-generated copper oxide nanoparticles were active in both assays and were found to be soluble in culture medium. Depletion of glutathione in the cells or loading the cells with ascorbate greatly increased heme oxygenase-1 induction in the presence of copper. By contrast, iron oxide nanoparticles were active in the phosphate-buffered saline but not in cell culture, and they aggregated in culture medium. Soluble salts of copper and iron exhibited the same contrast in activities as the respective combustion-generated particles. The results suggest that the capability of combustion-generated environmental samples to produce oxidant stress can be screened effectively in a two step process, first in phosphate-buffered saline with ascorbate and subsequently in epithelial cell culture for those exhibiting activity initially. The results also point to an unanticipated interaction in cells of oxidant stress-generating metals with an antioxidant (ascorbate) that is usually missing in culture medium formulations. Thus, ascorbate supplementation of cultured human cells is likely to improve their ability to model the in vivo effects of particulate matter containing copper and other redox-active metals.

1. Introduction

Metal oxide nanoparticles are of great interest in nanotechnology, in part because the family of metal oxides offers intriguing new properties for applications in future technologies. Copper oxide, for example, can be used to dope other materials for photocatalysis [1], can be added to fluids to create novel thermal properties as a so-called nanofluid [2,3], can aid in the synthesis of fullerenes [4], and can be used in energetic materials such as explosives and propellants [5]. Nanoparticles of iron oxide have been investigated as agents for cancer therapy with hyperthermia [6] induced by high frequency magnetic fields. They can also be used as a contrast agent for imaging. Engines, furnaces, smelters, and other high-temperature processes have the ability to emit ultrafine particles of iron and copper oxides into the atmosphere [7,8]. With its oxides being ubiquitous in the environment, iron is the most abundant of the transition metals emitted into the atmosphere, for example, in diesel engine soot [9]. Copper is also found in ambient aerosols, including in the ultrafine fraction, and can generate persistent free radicals upon exposure to aromatics at high temperature [10].

Exposure to nanoparticles typically occurs to epithelia of the lung, skin or gastrointestinal tract. Redox-active iron and copper ions are required cofactors for numerous critical intracellular enzymes and hence are essential for life. However, because of their propensity to generate reactive oxygen species, organisms have developed intricate pathways to regulate their intake and intracellular disposition [11,12]. Genetic defects in such regulation lead to well known diseases from which much has been learned about the pathology of iron and copper deficiency or excess [13,14]. Even

Abbreviations: BSO, buthionine sulfoximine; DHA, dehydroascorbate; DSF, desferoxamine; HO, hydroxyl radical; HO1, heme oxygenase-1; PBS, phosphate-buffered saline; *p*-HBA, *para*-hydroxybenzoate; SIK, spontaneously immortalized keratinocytes.

* Corresponding author at: Department of Environmental Toxicology, University of California, Davis, CA 95616-8588, United States. Tel.: +1 530 752 5176; fax: +1 530 752 3394.
E-mail address: rhrice@ucdavis.edu (R.H. Rice).

0009-2797/$ – see front matter © 2009 Elsevier Ireland Ltd. All rights reserved.
doi:10.1016/j.cbi.2009.08.007

normal levels of these metals have been hypothesized to contribute to oxidative processes in aging, including neurodegenerative and atherosclerotic disease [15]. Thus, the potential exposure of human populations and other living systems [16,17] to the uncontrolled release of nanoparticles from the manufacture and application of these materials, as well as exposure to nanoparticles that are emitted unintentionally during high-temperature processes such as combustion, has caused concern. Many studies have examined lung epithelial cell toxicology as a result of exposure to nanoparticles. As a target cell showing general responses among epithelia, human epidermal cells are examined in the present study.

Keratinocytes express high levels of heme oxygenase-1 (HO1), the major heme-degrading enzyme in mammals. This enzyme is induced not only by heme but also by a variety of metals, xenobiotics, pharmaceuticals and endocrine factors [18,19]. Its induction is part of an adaptive response to oxidative stress [20] reflecting the coordinate regulation of a group of oxidative stress-inducible genes by the Nrf2 transcription factor [21] that have a protective function in a variety of cell types including keratinocytes [22]. Nrf2 is rapidly degraded until electrophiles or oxidants increase its stability and transcriptional activity [23]. In degrading excess heme, such as that generated by hemoglobin turnover, HO1 produces biliverdin, ferrous ion (quickly incorporated into ferritin) and carbon monoxide. Biliverdin and the product into which it is converted, bilirubin, are potential antioxidants and, together with signaling by carbon monoxide, they can protect against oxidant stress and inflammation in tissues such as lung [24,25]. HO1 is a sensitive biomarker for activation of Nrf2 in the epidermis, essential for tumor prevention [26].

Cell defenses to oxidant stress include antioxidants such as glutathione and ascorbic acid (vitamin C). Intracellular ascorbic acid is capable of protecting glutathione-depleted cells from oxidants [27], but it is omitted from many cell culture medium formulations due to its generation of extracellular reactive oxygen [28]. Cultured cells can be sensitized to chromate-mediated DNA damage by supplementation with dehydroascorbate, which is reduced to ascorbate after uptake by the cells, thereby minimizing generation of reactive oxygen in the medium [29]. Despite its ability to act as an antioxidant, ascorbate can also act as a pro-oxidant by donating electrons to transition metals, which in turn can generate hydroxyl radicals in surrogate lung fluid solutions [30]. These observations suggested that modulation of the response of cells by ascorbate to other redox-active agents would merit investigation. This vitamin is particularly appropriate for keratinocytes, since it enhances the differentiation of cultured epidermal cells [31,32], and its use may improve the ability of the cultures to model responses in vivo.

2. Materials and methods

2.1. Generation and characterization of nanoparticles

Copper and iron oxide nanoparticles were synthesized in the gas phase by introducing the vapor of a metal precursor into a hydrogen/air diffusion flame. The flame was stabilized on a 3/8 in. stainless steel tube and located in a vertical wind tunnel. The equipment used in this study and the method for iron oxide particle synthesis are described in detail elsewhere [33]. For iron oxide, the H_2 flow rate was 1.0 L/min. A portion of the H_2 stream was diverted and bubbled through liquid iron pentacarbonyl, maintained at 0 °C, at a rate of 10 cm^3/min. For the synthesis of copper oxide particles, the fuel stream consisted of a 1:1 mixture of H_2 and N_2 at a flow rate of 1.5 L/min. The entire fuel stream was passed through a cartridge containing copper acetylacetonate maintained at 160 °C and located just below the exit of the flame holder.

Particles in the flame effluent were sampled using a vacuum probe and collected on polytetrafluoroethylene membrane filters (Advantec Inc.) with a pore size of 0.2 μm. The aerosol size distribution at the sampling location was measured using a scanning mobility particle sizer (TSI, Inc.). Particle size and morphology were observed using a Phillips CM-12 transmission electron microscope. The particle crystal phase was identified using a Scintag powder X-ray diffractometer. The nanoparticles were generated in an enclosed facility with the particle stream enclosed in a large volume of co-flowing clean air. Particle concentrations in the laboratory were monitored with a scanning mobility particle sizer. After collection, the particles were handled in a fume hood and kept in a sealed container until delivery to the cell culture facility.

Dialysis membranes were utilized to determine the dissolution of copper oxide nanoparticles in cell culture medium. Stock particle suspensions of 5 mg/mL were prepared in a 1:1 mixture of Dulbecco-Vogt Eagle's and Ham's F12 media (Caisson Laboratories, North Logan, UT). Particle suspension aliquots of 200 μL were placed in miniature dialysis units (Pierce Biotech) manufactured with 3500 MW cut-off membranes that allowed the passage of dissolved Cu ions but not CuO nanoparticles into the dialysate. Each dialysis unit was floated in 5 mL of particle-free medium at room temperature. The dialysate was not shaken or stirred during the experiment. After removal of the dialysis units at selected time points, the concentration of dissolved copper in the dialysate was measured by a calibrated spectrophotometric method using oxalic acid bis(cyclohexylidene hydrazide) as a copper chelating agent [34]. Absorbance of the copper-cuprizone complex was measured at 600 nm.

2.2. Assay of hydroxyl radical generation in cell-free phosphate-buffered saline

The generation of hydroxyl radical (OH) by dissolved or particulate metals in phosphate-buffered saline (PBS) was determined using a benzoate probe [30], which quantitatively traps OH and converts it to *para*-hydroxybenzoate (*p*-HBA). We used a cell-free, air saturated, PBS solution consisting of 10 mM sodium benzoate (to trap OH), 114 mM sodium chloride, and 10 mM phosphate (7.8 mM Na_2HPO_4 and 2.2 mM KH_2PO_4) to buffer the solution at pH 7.4. Prior to use, PBS solutions were treated with Chelex-100 resin to remove metals. Where applicable, stock solutions of ascorbate and citrate were prepared fresh and added to the Chelex-treated PBS on the day of each experiment.

OH generation by dissolved Fe(III) and Cu(II) was measured by adding 10 mL of PBS (and, where applicable, 200 μM ascorbate or 300 μM citrate) to a series of 125-mL Teflon bottles, adding 20 μM of freshly prepared metal solution ($FeCl_3$ or $CuCl_2$) to the series, wrapping the bottles with aluminum foil to keep them dark, and shaking. After a given amount of time (0–24 h), we removed one bottle from the series, added 100 μM desferoxamine (DSF) and 50 μM HSO_3^- to stop the generation of OH, acidified the solution to pH 2 with 100 μL of 1.0 M H_2SO_4, filtered it with a 0.22 μm pore syringe filter (Millex GP, Millipore) and injected onto a reverse-phase HPLC with UV–vis detection to quantify the *p*-HBA concentration. Concentrations of *p*-HBA were converted to OH concentrations based on (1) the fraction of OH in our system that reacts with benzoate (98%) and (2) the yield of *p*-HBA from the reaction of OH with benzoate (21.5%) [30]. OH generation by nanoparticulate Fe or Cu was measured in a similar way as for the dissolved metals. Particles collected on polytetrafluoroethylene filters were placed into foil-covered Teflon bottles containing PBS (with the particle side face down in the solution) and the bottles were shaken for 24 h. At the end of the extraction, DSF and HSO_3^- were added (to prevent further OH generation) and the solution was acidified, filtered, and then injected into the HPLC. Concentrations of Fe and Cu

in the PBS after 24 h of shaking were determined by first passing the solutions thorough a 0.22 μm filter, then diluting 1:10 with 3% HNO_3 and analyzing them with an Agilent 7500ce ICP quadrupole mass spectrometer.

2.3. Cell culture

Spontaneously immortalized human keratinocytes (SIK) [35], passages 22–31, were cultured with support of a lethally irradiated feeder layer of 3T3 fibroblasts in a 2:1 mixture of DMEM and F12 media supplemented with fetal bovine serum (5%), hydrocortisone (0.4 μg/mL), insulin (5 μg/mL), transferrin (μg/mL), triiodothyronine (20 pM), adenine (0.18 mM) and, starting at the first medium change, epidermal growth factor (10 nM). In some experiments, cultures were pretreated overnight (16 h) with 0.5 mM buthionine sulfoximine (BSO) in serum free medium, which lowered the glutathione concentration to 34 ± 7% of the normal resting level. When indicated, dehydroascorbate (DHA) at 2 mM was added to the newly confluent cultures for 1 h prior to addition of copper or iron compounds. In preliminary trials, induction of HO1 after metal treatment was nearly maximal after 8 h (double that at 4 h) and was only marginally higher after 24 h. Combustion particles were suspended and sonicated in serum free medium immediately prior to addition to the cultures. Copper oxide particulates were not visible through the culture microscope, but considerable aggregation of the iron particles was evident. The cultures displayed pyknotic nuclei, a general symptom of toxicity, at a copper concentration of 750 μM, but the morphological appearance was normal at the much lower concentrations, all <100 μM, used in other experiments.

2.4. Real-time reverse transcriptase polymerase chain reaction

Total RNA was isolated using TRIzol reagent (Invitrogen, Carlsbad, CA). To avoid amplification of genomic DNA, RNA was pretreated with DNase (DNA-free kit, Ambion, Austin, TX). cDNA synthesis was performed using a High Capacity cDNA Archive Kit (Applied Biosystems, Foster City, CA). The cDNA served as a template in quantitative real-time PCR performed in an ABI 7500 Fast Sequence Detection System utilizing TaqMan Fast Universal PCR Master Mix and TaqMan Gene Expression assay probes for HO1 and the housekeeping genes β_2-microglobulin and β-glucuronidase (Applied Biosystems). Normalization by the $\Delta\Delta C_t$ method [36] is illustrated with normalization to β-glucuronidase, but equivalent results were obtained using β_2-microglobulin. C_t values for uninduced HO1 (without treatments) were 29.3 ± 1.4; C_t values for β-glucuronidase and β_2-microglobulin were 24.8 ± 0.3 and 20.7 ± 0.2, respectively, and did not change significantly with treatments. The data were analyzed as blocked ANOVA models, blocking by the experiment. All analyses were done using SAS (version 9.1). All responses were log transformed to satisfy the normality and constant variance assumptions. *Post hoc* comparisons against control treatments were done based on least squares means, using Dunnett's method. Results were considered significant whenever $p < 0.05$.

3. Results

3.1. Characterization of combustion-generated nanoparticles

The iron oxide particles, prepared as previously described [33] and illustrated [37], consisted of two size modes with mean diameters estimated by transmission electron microscopy of 3–8 nm and ≈45 nm, respectively. The crystal structure and iron valence state corresponded to maghemite (γ-Fe_2O_3). A sample transmission electron micrographic image of copper oxide nanoparticles is given in Fig. 1A. Aggregate or chain-like particles were formed

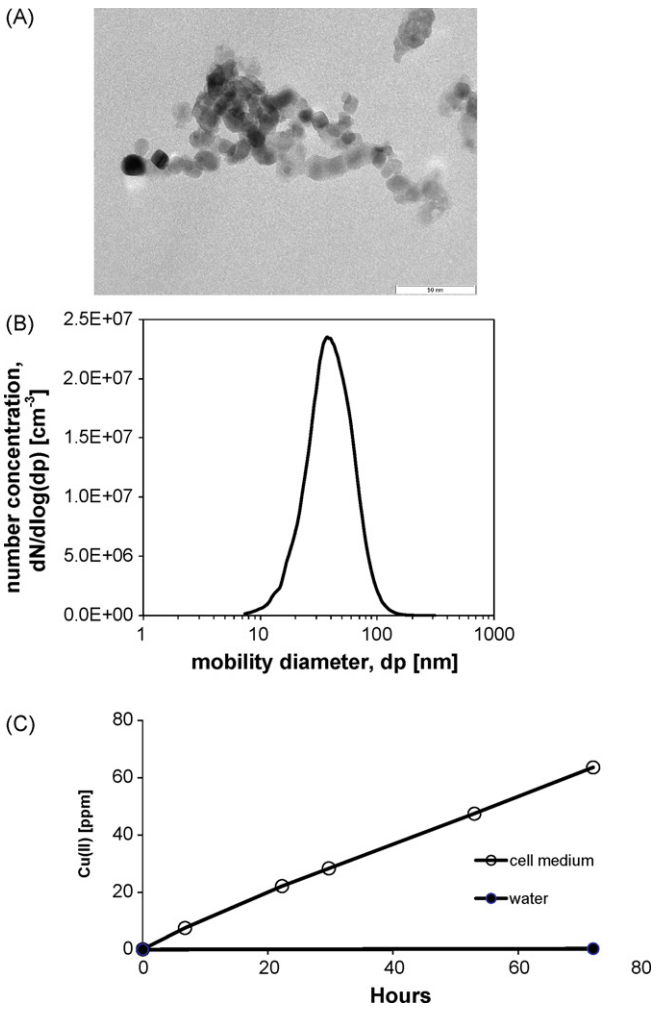

Fig. 1. Properties of copper oxide nanoparticles. (A) Electron micrograph of a small sample of the particles after drying the suspension on the microscope grid, which induced aggregation. Scale bar = 50 nm. (B) Size distribution of the particles in the flame effluent. (C) Comparison of solubilization in water or cell culture medium as indicated.

by the agglomeration of smaller particles, which become sintered together in the high-temperature flame environment. The aerosol size distribution, as measured by the scanning mobility particle sizer and shown in Fig. 1B, was log-normal with a count mean mobility diameter of 43 nm. X-ray diffraction analysis revealed the presence of only one crystal phase, corresponding to monoclinic CuO. When these particles were added to cell culture medium, they appeared to dissolve to a greater extent than anticipated from the known water solubility of CuO. Fig. 1C shows this quantitatively; while the combustion-generated CuO nanoparticles dissolved rapidly in culture medium, they dissolved at a negligible rate in water.

3.2. Generation of hydroxyl radicals by soluble Fe and Cu

To examine the ability of aqueous iron or copper to generate reactive oxygen species in the absence of cells, and to determine how ascorbate affects this chemistry, we measured the formation of hydroxyl radical (OH) by Fe(III) and Cu(II) in cell-free PBS. As shown in Fig. 2, neither Fe nor Cu forms any substantial amount of OH in the PBS solution alone, and the addition of citrate to PBS has a negligible effect. In contrast, the addition of ascorbate to the PBS greatly increases the formation rate of OH in both the Fe and Cu solutions. Compared to the PBS baseline condition, adding ascor-

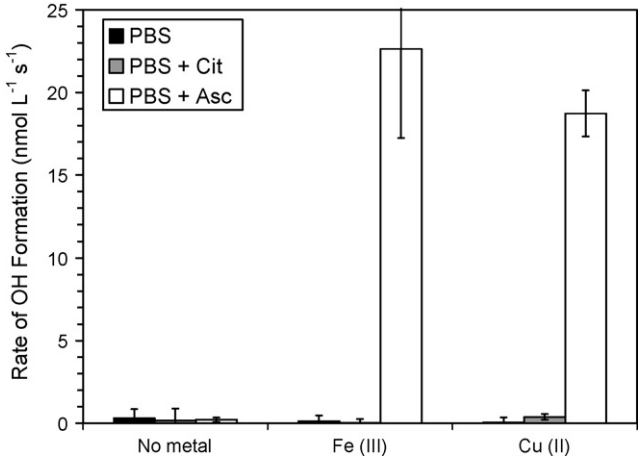

Fig. 2. Rates of hydroxyl radical (OH) formation by 20 μM of aqueous $FeCl_3$ or $CuCl_2$ in cell-free, phosphate-buffered saline (PBS) with and without citrate (Cit, 300 μM) or ascorbate (Asc, 200 μM). Error bars represent 95% confidence intervals.

bate increased the rate of OH formation by a factor of ≈200 for both the Fe and Cu solutions. It is difficult to determine the exact factors because the rates of OH formation in PBS (without ascorbate) for both Fe and Cu are not statistically different from zero; thus the factor of 200 likely underestimates the true impact of ascorbate on OH generation by these metals. Although the production rate of OH from dissolved Fe is 20% higher than that from dissolved Cu, this difference is not statistically significant (Fig. 2).

Fig. 3 shows that OH is also generated from both the Fe and Cu nanoparticles in PBS containing both ascorbate and citrate. Whether the OH response is normalized by the total PM mass collected on the filters (Fig. 3A), or the amount of dissolved Fe or Cu measured in the PBS after extraction (Fig. 3B), the relative response from the two nanoparticulate metals is similar, with iron generating roughly 3–6 times more OH than copper.

The generation of hydroxyl radical in these solutions most likely occurs by the following sequence [30]: (1) reduction of the oxidized form of the metal by ascorbate, (2) transfer of the electron from the reduced metal to dissolved oxygen to form superoxide, (3) formation of hydrogen peroxide by transfer of an electron from another reduced metal to superoxide, and (4) OH formation via the Fenton reaction (or a Fenton-like reaction in the case of copper). For iron solutions this sequence is:

$$\mathrm{Fe(III) + Asc \rightarrow Fe(II) + products} \quad (1)$$

$$\mathrm{Fe(II) + O_2 \rightarrow Fe(III) + {}^{\bullet}O_2^{-}} \quad (2)$$

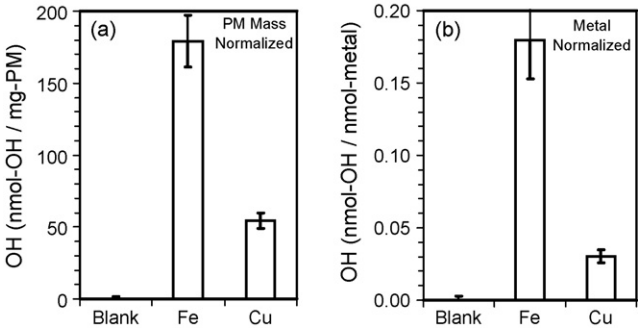

Fig. 3. Amounts of hydroxyl radical (OH) formed after 24 h of extraction of Fe and Cu nanoparticles collected on Teflon filters. Samples were extracted in cell-free PBS containing 300 μM citrate and 200 μM ascorbate. Results in panel (A) are normalized to the total mass of particles collected on each filter, while results in panel (B) are normalized to the measured concentration of Fe or Cu in the PBS solution at the end of filter extraction. Error bars represent ±1 standard deviation.

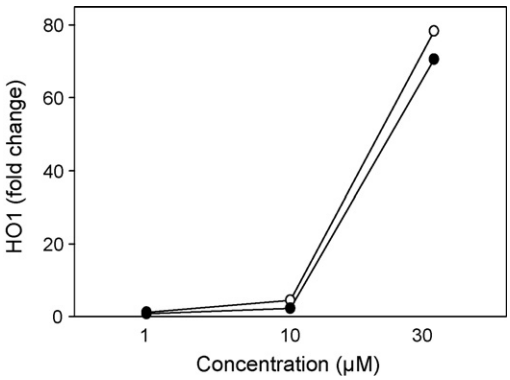

Fig. 4. Concentration dependence of heme oxygenase-1 (HO1) induction after exposure to copper oxide nanoparticles (●) or copper sulfate solution (○) at the indicated concentrations. The result shown is representative of three experiments.

$$\mathrm{Fe(II) + {}^{\bullet}O_2^{-} + 2H^{+} \rightarrow Fe(III) + HOOH} \quad (3)$$

$$\mathrm{Fe(II) + HOOH \rightarrow Fe(III) + OH + OH^{-}} \quad (4)$$

As shown by these reactions, OH formation from dissolved O_2 requires three sequential electron transfers from a reductant via the transition metal. Fig. 2 shows that citrate is unable to appreciably reduce Fe(III) or Cu(II) over the 24 h of our experiments, but that ascorbate can very rapidly reduce/cycle these metals and produce substantial amounts of hydroxyl radical.

3.3. Response of keratinocyte cultures

Treatment of SIK cultures with copper oxide nanoparticles from combustion samples (which dissolved to yield the given concentrations) resulted in induction of HO1 mRNA in a dose dependent manner. Initial experiments with overnight exposure (16 h) showed nearly a doubling of HO1 mRNA at 6 μM and maximal induction of ≈1000-fold at ≥150 μM added copper nanoparticles. Subsequent experiments employed more environmentally relevant copper concentrations (less than 100 μM) and treatment times of 8 h. Under these conditions, the concentration dependence of HO1 induction was found to be essentially the same for copper oxide nanoparticles and copper sulfate as shown in Fig. 4, where HO1 mRNA monotonically increased with the concentration of either agent. In initial experiments, cuprous chloride elicited nearly the same response as cupric sulfate and was not studied further.

To increase the sensitivity of HO1 induction measurements, the culture medium was supplemented with BSO (an inhibitor of glutathione synthesis) and/or DHA (taken up and reduced to ascorbic acid). Concentration dependence experiments with copper sulfate, shown in Fig. 5, showed that BSO permitted a marked induction of HO1 mRNA at the highest concentration of copper employed (30 μM), as did DHA, but the latter also sensitized the cells to an order of magnitude lower copper concentration. The combination of BSO and DHA produced a substantial increase in HO1 induction compared to cultures with either agent alone or with neither agent. As shown in Fig. 5, a significant response was detected down to the lowest copper concentrations employed in cultures treated with DHA + BSO, whereas a significant response was detected only at the highest copper concentration in the absence of DHA.

As shown in Fig. 6A, consistent with the above experiments with copper sulfate, BSO and DHA also sensitized the cells to CuO nanoparticles. In contrast, iron combustion-generated nanoparticles applied to the cell cultures produced little HO1 induction. The iron particles formed microscopically obvious clumps in the medium, so it was unclear how much exposure to iron the cells experienced. To find whether iron in a soluble state was effective in such induction, ferrous or ferric salts were added to the culture

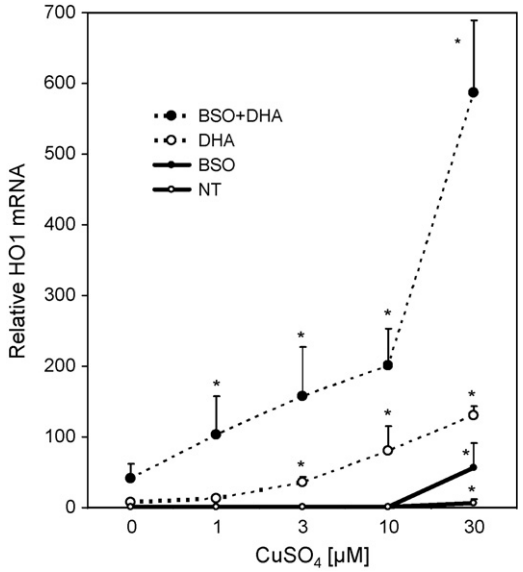

Fig. 5. Induction of heme oxygenase-1 (HO1) in keratinocyte cultures by the indicated concentration of $CuSO_4$ after 8 h of exposure. Cultures were treated with buthionine sulfoximine (BSO) and/or dehydroascorbate (DHA) or neither (NT) as indicated, followed by measurement of relative levels of HO1 mRNA by real-time PCR. Values illustrated are the means and standard deviations of three experiments. For each condition (NT, BSO, DHA, BSO + DHA), the asterisks indicate values significantly different ($p < 0.05$) from those from cultures not treated with $CuSO_4$.

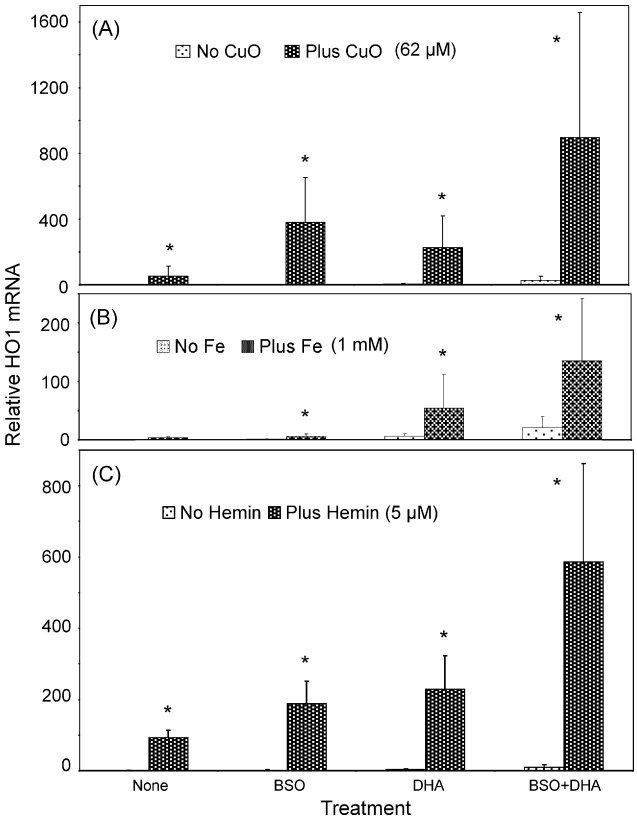

Fig. 6. Induction of heme oxygenase-1 (HO1) by (A) copper oxide nanoparticles (62 μM CuO), (B) 1 mM ferric nitrate (Fe) or (C) 5 μM hemin after 8 h of exposure. Cultures were treated with combinations of the indicated compound, buthionine sulfoximine (BSO) and/or dehydroascorbate (DHA) as indicated, followed by measurement of relative levels of HO1 mRNA by real-time PCR. Values illustrated are the means and standard deviations of three or four experiments. *Post hoc* comparisons were done using a Bonferroni adjustment for the four within-treatment comparisons in each graph. Asterisks show HO1 induction levels significantly above those detected in cultures without CuO, Fe or hemin treatment, respectively. In each case, the value with CuO, Fe or hemin was compared to the control with same treatment (±BSO and ±DHA).

medium. These were almost totally ineffective in inducing HO1. In the presence of BSO and DHA, the stimulation was noticeable only in cultures with concentrations of 0.1–1 mM. Fig. 6B shows an induction by ferric nitrate of ≈5-fold over background induction in cells treated with DHA ± BSO. A similar degree of stimulation was noted with 0.1 mM ferric nitrate. Iron in the form of hemin, the iron-containing protoporphyrin IX of heme proteins, is a powerful general inducer of HO1, including in keratinocytes as previously shown [38]. Present work (Fig. 6C) demonstrates this effect, where BSO and DHA exhibited stimulatory action separately and together.

4. Discussion

The present experiments provide two ways to characterize possible oxidant stress by metal oxide nanoparticles. First, measurement of hydroxyl radicals generated under cell-free conditions shows the potential for cellular damage. A critical component of such measurement is ascorbate, a ubiquitous antioxidant in mammalian cells. Ascorbate has long been known to exhibit antioxidant or pro-oxidant character depending on the circumstances. Results with the second approach, where the response of cultured keratinocytes to copper was dramatically increased by loading them with DHA, indicate the relevance of ascorbate to cell-based bioassays. However, responses of intact cells also reflect their defenses. The findings indicate, as studies have shown with many cell types, that depleting keratinocytes of glutathione provides a sensitization to oxidative stress. While the cells were highly responsive to copper ions, and where sensitization has utility for detecting oxidative stress, they were poorly responsive to iron. A dramatically higher potency of copper compared to iron was also observed in their abilities to induce pulmonary inflammation in rat lung [39] and mouse lung [17], to induce cytokine production in cultured human BEAS-2B cells [40] and to give toxicity in three immortalized lung derived cell lines in culture [41]. Complementing ongoing epidemiological and source apportionment studies [8], a first screen of environmental samples using synthetic fluid – such as described here – likely will eliminate biologically inactive ones, and those exhibiting activity can then be subjected to more discriminating testing in cell culture.

The lack of response by the keratinocytes to ferric or ferrous salts alone added to the medium likely reflects low iron uptake by the transferrin-mediated route [42]. The culture medium had an estimated transferrin concentration of 2–3 μM derived from serum, suggesting an iron concentration of ≈5 μM available for uptake. Hepatocytes exhibit nontransferrin-mediated uptake of iron, a concern in patients with iron overload and elevated plasma levels [43], but the keratinocytes did not display adverse effects even at very high medium concentrations. Nevertheless, they did respond to iron treatment in the presence of BSO and DHA with elevated HO1 induction, probably as a consequence of a small increase in the intracellular pool of labile iron not bound to ferritin [44]. Such a pool of transition metals could be responsible for the increase in HO1 seen with these additions but without added copper or iron, consistent with the present observation of hydroxyl radical generation in PBS with added ascorbate.

The dramatic HO1 induction in cells by copper reflects the lack of such an effective limit on uptake. In addition to uptake by the ubiquitously expressed Ctr1 transporter, with a Km of ≈1 μM for cuprous ion, mammalian cells can exhibit other transport systems, including a distinct one with Km of ≈10 μM for cupric ion [45]. Such a high Km pathway may be relevant in the present case since, as shown in Fig. 4, the concentration dependence of induc-

tion was nonlinear; a concentration of 30 μM exhibited a much higher induction in HO1 than one of 10 μM. Depletion of cellular antioxidant defense at the higher concentrations would be consistent with the effect of depleting glutathione in the cells using BSO or adding DHA. In the presence of the excessive copper concentrations encountered in these experiments, export from the cells (e.g., by the ATP7B pump) evidently did not keep up with intake.

Ascorbate has been hypothesized to augment the DNA damage caused by intracellular Cr(VI) by providing a unique two electron reduction contributing to its conversion to Cr(III), where the resulting DNA damage is not a consequence of the generation of oxidative stress [46]. Consistent with this interpretation, the present experiments confirmed our previous findings that 3 μM chromate, which suppresses keratinocyte differentiation, has little if any ability to induce HO1 [38]. Moreover, BSO and DHA treatment exhibited no added sensitization of the cells to chromate (data not shown). On the other hand, the simplest explanation for the dramatic effect of DHA on the cellular response to copper ions is an increase in redox cycling that stabilizes Nrf2 and increases its transcriptional activity. Increased reduction of cuprate to cuprous ion at the cell surface to permit faster entry appears unlikely, since the cells exhibited essentially the same sensitivity to cuprous and cupric ion in preliminary experiments.

Concern about the biological effects of nanoparticles derives in part from their high ratio of surface area to mass. As a consequence, more of the molecules in a dose of a given mass can participate in interactions with their cellular environment. In addition, however, nanoparticles may interact more readily with their aqueous environment, resulting in accelerated dissolution. Although not expected to dissolve in water at the highest concentrations applied to the cultures, the CuO nanoparticles readily dissolved in culture medium, probably through the influence of ligands such as amino acids and other components typical of the cellular microenvironment. This aspect of the physical properties of nanoparticles must be taken into account to understand their biological activities. In addition, the value of assays for cellular response is enhanced by increased sensitivity and by mimicking the cellular microenvironment in vivo. Supplementing culture medium with an inhibitor of glutathione synthesis (BSO) and a redox-active nutrient that is generally missing (ascorbate as DHA) helps accomplish these objectives. The present approach is anticipated to permit improved screening of nanoparticles and other samples for oxidant effects as a guide to animal studies or epidemiological analyses.

Conflict of interest statement

None.

Acknowledgments

We thank Dr. Alan Buckpitt for glutathione measurements and review of the manuscript and Dr. Kent Pinkerton for valuable discussion. This publication was supported by grant 5 P42 ES004699 from the National Institute of Environmental Health Sciences (NIEHS). The contents are solely the responsibility of the authors and do not represent the official views of the NIEHS.

References

[1] K.X. Song, J.H. Zhou, J.C. Bao, Y.Y. Feng, Photocatalytic activity of (copper, nitrogen)-codoped titanium dioxide nanoparticles, J. Am. Ceram. Soc. 91 (2008) 1369–1371.
[2] S. Khandekar, Y.M. Joshi, B. Mehta, Thermal performance of closed two-phase thermosyphon using nanofluids, Int. J. Therm. Sci. 47 (2008) 659–667.
[3] N.R. Karthikeyan, J. Philip, B. Raj, Effect of clustering on the thermal conductivity of nanofluids, Mater. Chem. Phys. 109 (2008) 50–55.
[4] D.F. Liu, S.H. Yang, S.T. Lee, Preparation of novel cuprous oxide-fullerene[60] core-shell nanowires and nanoparticles via a copper(I)-assisted fullerene-polymerization reaction, J. Phys. Chem. C 112 (2008) 7110– 7118.
[5] R. Shende, S. Subramanian, S. Hasan, S. Apperson, R. Thiruvengadathan, K. Gangopadhyay, S. Gangopadhyay, P. Redner, D. Kapoor, S. Nicolich, W. Balas, Nanoenergetic composites of CuO nanorods, nanowires, and Al-nanoparticles, Propell. Explos. Pyrot. 33 (2008) 122–130.
[6] Q. Zeng, I. Baker, J.A. Loudis, Y. Liao, P.J. Hoopes, J.B. Weaver, Fe/Fe oxide nanocomposite particles with large specific absorption rate for hyperthermia, Appl. Phys. Lett. 90 (2007) 233112.
[7] N. Bukowiecki, R. Gehrig, M. Hill, P. Lienemann, C. Zwicky, B. Buchmann, E. Weingartner, U. Baltensperger, Iron, manganese and copper emitted by cargo and passenger trains in Zurich (Switzerland): size-segregated mass concentrations in ambient air, Atmosph. Environ. 41 (2007) 878–889.
[8] R.M. Duvall, G.A. Norris, L.A. Dailey, J.M. Burke, J.K. McGee, M.I. Gilmour, T. Gordon, R.B. Devlin, Source apportionment of particulate matter in the US and associations with lung inflammatory markers, Inhal. Toxicol. 20 (2008) 671–683.
[9] F.E. Huggins, G.P. Huffman, J.D. Robertson, Speciation of elements in NIST particulate matter SRMs 1648 and 1650, J. Hazard. Mater. 74 (2000) 1–23.
[10] S. Lomnicki, H. Truong, E. Vejerano, B. Dellinger, Cooper oxide-based model of persistent free radical formation on combustion-derived particulate matter, Environ. Sci. Technol. 42 (2008) 4982–4988.
[11] L. Dunn, Y.S. Rahmanto, D.R. Richardson, Iron uptake and metabolism in the new millenium, Trends Cell Biol. 17 (2007) 93–100.
[12] B.E. Kim, T. Nevitt, D.J. Thiele, Mechanisms for copper acquisition, distribution and regulation, Nat. Chem. Biol. 4 (2008) 176–185.
[13] E.L. Mackenzie, K. Iwasaki, Y. Tsuji, Intracellular iron transport and storage: from molecular mechanisms to health implications, Antiox. Redox Signal. 10 (2008) 997–1030.
[14] I.G. Macreadie, Copper transport and Alzheimer's disease, Eur. Biophys. J. 37 (2008) 295–300.
[15] G.J. Brewer, Iron and copper toxicity in diseases of aging, particularly atherosclerosis and Alzheimer's disease, Exp. Biol. Med. 232 (2007) 323–335.
[16] M. Heinlaan, A. Ivask, I. Blinova, H.C. Dubourguier, A. Kahru, Toxicity of nanosized and bulk ZnO, CuO and TiO_2 to bacteria *Vibrio fischeri* and crustaceans *Daphnia magna* and *Thamnocephalus platyurus*, Chemosphere 71 (2008) 1308–1316.
[17] H. Prieditis, I.Y.R. Adamson, Comparative pulmonary toxicity of various soluble metals found in urban particulate dusts, Exp. Lung Res. 28 (2002) 563–576.
[18] C. Li, P. Hossieny, B.J. Wu, A. Qawasmeh, K. Beck, R. Stocker, Pharmacological induction of heme oxygenase-1, Antiox. Redox Signal. 9 (2007) 2227–2239.
[19] N.G. Abraham, A. Kappas, Pharmacological and clinical aspects of heme oxygenase, Pharmacol. Rev. 60 (2008) 79–127.
[20] S.W. Ryter, A.M.K. Choi, Heme oxygenase-1: molecular mechanisms of gene expression in oxygen-related stress, Antiox. Redox Signal. 4 (2002) 625–632.
[21] T. Ishii, K. Itoh, S. Takahashi, H. Sato, T. Yamagawa, Y. Katoh, S. Bannai, M. Yamamoto, Transcription factor Nrf2 coordinately regulates a group of oxidative stress-inducible genes in macrophages, J. Biol. Chem. 275 (2000) 16023–16029.
[22] T.A. Beyer, U. auf dem Keller, S. Braun, M. Schafer, S. Werner, Roles and mechanisms of action of the Nrf2 transcription factor in skin morphogenesis, wound repair and skin cancer, Cell Death Differ. 14 (2007) 1250–1254.
[23] T. Nguyen, P. Nioi, C.B. Pickett, The Nrf-2 antioxidant response element signaling pathway and its activation by oxidative stress, J. Biol. Chem. 284 (2009) 13291–13295.
[24] E.P. Carter, C. Garat, M. Imamura, Continual emerging roles of HO-1: protection against airway inflammation, Am. J. Physiol. Lung Cell. Mol. Physiol. 287 (2004) L24–L25.
[25] L.E. Fredenburgh, M.A. Perrella, S.A. Mitsialis, The role of heme oxygenase-1 in pulmonary disease, Am. J. Respir. Cell Mol. Biol. 36 (2007) 158–165.
[26] U. Auf dem Keller, M. Huber, T.A. Beyer, A. Kumin, C. Siemes, S. Braun, P. Bugnon, V. Mitropoulos, D.A. Johnson, J.A. Johnson, D. Hohl, S. Werner, Nrf transcription factors in keratinocytes are essential for skin tumor prevention but not for wound healing, Mol. Cell. Biol. 26 (2006) 3773–3784.
[27] V.H. Guaniquil, J.C. Vera, D.W. Golde, Mechanism of vitamin C inhibition of cell death induced by oxidative stress in glutathione-depleted HL-60 cells, J. Biol. Chem. 276 (2001) 40955–40961.
[28] M.-V. Clement, J. Ramalingam, L.H. Long, B. Halliwell, The in vitro cytotoxicity of ascorbate depends on the culture medium used to perform the assay and involves hydrogen peroxide, Antiox. Redox Signal. 3 (2001) 157–163.
[29] M. Reynolds, L. Stoddard, I. Bespalov, A. Zhitkovich, Ascorbate acts as a highly potent inducer of chromate mutagenesis and clastogenesis: linkage to DNA breaks in G2 phase by mismatch repair, Nucleic Acids Res. 35 (2007) 465–476.
[30] E. Vidrio, H. Jung, C. Anastasio, Generation of hydroxyl radicals from dissolved transition metals in surrogate lung fluid solutions, Atmosph. Environ. 42 (2008) 4369–4379.
[31] S.T. Boyce, A.P. Supp, V.B. Swope, G.D. Warden, Vitamin C regulates keratinocyte viability, epidermal barrier, and basement membrane in vitro, and reduces wound contraction after grafting of cultured skin substitutes, J. Invest. Dermatol. 118 (2002) 565–572.

[32] I. Savini, M.V. Catani, A. Rossi, G. Duranti, G. Melino, Characterization of keratinocyte differentiation induced by ascorbic acid: protein kinase C involvement and vitamin C homeostasis, J. Invest. Dermatol. 118 (2002) 372–379.
[33] B. Guo, I.M. Kennedy, Gas-phase flame synthesis and characterization of iron oxide nanoparticles for use in a health effects study, Aerosol Sci. Technol. 41 (2007) 944–951.
[34] C.U. Wetlesen, Rapid spectrophotometric determination of copper and in iron, steel, and ferrous alloys, Analyt. Chim. Acta 16 (1957) 268–270.
[35] R.H. Rice, K.E. Steinmann, L.A. deGraffenried, Q. Qin, N. Taylor, R. Schlegel, Elevation of cell cycle control proteins during spontaneous immortalization of human keratinocytes, Mol. Biol. Cell 4 (1993) 185–194.
[36] M.L. Wong, J.F. Medrano, Real-time PCR for mRNA quantitation, BioTechniques 39 (2005) 75–85.
[37] A. Gojova, B. Guo, R.S. Kota, J.C. Rutledge, I.M. Kennedy, A.I. Barakat, Induction of inflammation in vascular endothelial cells by metal oxide nanoparticles: effect of particle composition, Environ. Health Perspect. 115 (2007) 403–409.
[38] M.A. Rea, J.P. Gregg, Q. Qin, M.A. Phillips, R.H. Rice, Global alteration of gene expression in human keratinocytes by inorganic arsenic, Carcinogenesis 24 (2003) 747–756.
[39] T.M. Rice, R.W. Clarke, J.J. Godleski, E. Al-Mutairi, N.-F. Jiang, R. Hauser, J.D. Paulauskis, Differential ability of transition metals to induce pulmonary inflammation, Toxicol. Appl. Pharmacol. 177 (2001) 46–53.
[40] T. Kennedy, A.J. Ghio, W. Reed, J.M. Samet, J. Zagorski, J. Quay, J. Carter, L.A. Dailey, J.R. Hoidal, R.B. Devlin, Copper-dependent inflammation and nuclear factor-kB activation by particulate air pollution, Am. J. Respir. Cell Mol. Biol. 19 (1998) 366–378.
[41] M.R. Riley, D.E. Boesewetter, R.A. Turner, A.M. Kim, J.M. Collier, A. Hamilton, Comparison of the sensitivity of three lung derived cell lines to metals from combustion derived particulate matter, Toxicol. In Vitro 19 (2005) 411–419.
[42] R.R. Crichton, S. Wilmet, R. Leggsyer, R.J. Ward, Molecular and cellular mechanisms of iron homeostasis and toxicity in mammalian cells, J. Inorg. Biochem. 91 (2002) 9–18.
[43] A.C.G. Chua, R.M. Graham, D. Trinder, J.K. Olynyk, The regulation of cellular iron metabolism, Crit. Rev. Clin. Lab. Sci. 44 (2007) 413–459.
[44] W. Breuer, M. Shvartsman, Z.I. Cabantchik, Intracellular labile iron, Int. J. Biochem. Cell Biol. 40 (2008) 350–354.
[45] J.B. Lee, M.J. Petris, D.J. Thiele, Characterization of mouse embryonic cells deficient in the Ctr1 high affinity copper transporter, J. Biol. Chem. 277 (2002) 40253–40259.
[46] M. Reynolds, A. Zhitkovich, Cellular vitamin C increases chromate toxicity via a death program requiring mismatch repair but not p53, Carcinogenesis 28 (2007) 1613–1620.